Development of a nomogram for predicting radiation-induced pneumonia in patients with lung cancer undergoing close-range radiotherapy with radioactive ^{125}I particles

TINGTING DING[1], SHANHU HAO[1], ZHIGUO WANG[1,2], WENWEN ZHANG[1,2] and GUOXU ZHANG[1,2]

[1]Department of Nuclear Medicine, General Hospital of Northern Theater Command, Shenyang, Liaoning 110016, P.R. China; [2]College of Medicine and Biological Information Engineering, Northeastern University, Shenyang, Liaoning 110167, P.R. China

Received June 19, 2024; Accepted September 25, 2024

DOI: 10.3892/mco.2024.2797

Abstract. The most common and potentially fatal side effect of postoperative radiotherapy using radioactive ^{125}I particles in the chest is radiation-induced pneumonia (RP). The present study aimed to develop a nomogram to accurately predict RP in patients with lung cancer following this type of radiotherapy. A retrospective analysis was conducted on data from 436 patients with advanced lung cancer who underwent close-range radiotherapy using radioactive ^{125}I particles at the General Hospital of Northern Theater Command from January 2016 to December 2023 (Shenyang, China). Risk factors for RP were identified through least absolute shrinkage and selection operator logistic regression and multivariable logistic regression analysis. These factors were then used to construct a dynamic nomogram. The predictive performance of the nomogram was validated using receiver operating characteristic (ROC) curves, calibration plots, and decision curve analysis. Additionally, the grading of RP and Kaplan-Meier analysis were performed. Preoperative N and M staging, the maximum dose and whether chemotherapy was administered were identified as significant predictors of RP. A dynamic nomogram for predicting RP was developed based on these risk factors. The area under the ROC curve was 0.878 (95% CI, 0.814-0.942) for the training cohort and 0.828 (95% CI, 0.787-0.870) for the validation cohort, indicating favorable discriminatory ability. The nomogram demonstrated excellent calibration. In both cohorts, the maximum dose parameter provided the most significant clinical benefits, supporting its promising clinical utility. Patients staged as T_1 and T_3 preoperatively were more likely to develop RP compared with those staged as T_2 (P<0.001). Likewise, patients staged as M_1 preoperatively, those receiving a maximum dose above the mean, and those who had undergone chemotherapy exhibited a higher probability of developing RP (P<0.001). The developed nomogram offers a precise and user-friendly tool for clinical application in predicting the risk of RP in patients with lung cancer undergoing close-range radiotherapy with radioactive ^{125}I particles.

Correspondence to: Dr Guoxu Zhang, Department of Nuclear Medicine, General Hospital of Northern Theater Command, 83 Wenhua Road, Shenhe, Shenyang, Liaoning 110016, P.R. China
E-mail: zhangguoxu502@sina.com

Abbreviations: RP, radiation-induced pneumonia; LASSO, least absolute shrinkage and selection operator; ROC, receiver operating characteristic; DCA, decision curve analysis; CT, computed tomography; PET-CT, positron emission tomography-computed tomography; ZPS, zymosan-activated serum; KPS, key performance indicator system; NRS, numeric rating scale; CEA, carcinoembryonic antigen; Nse, neuron-specific enolase; SCC, squamous cell carcinoma; PTV, planned target volume; D90, diameter at 90% cumulative volume; V100, volume at 100% cumulative volume; OS, overall survival

Key words: radioactive ^{125}I particles, close-range radiotherapy, RP, nomogram model

Introduction

Radioactive particles are small rods composed of sealed radioactive isotopes encased within metal shells, measuring 0.8 mm in diameter and 4.5 mm in length, with a half-life of 59.6 days (1). Close-range radiotherapy using radioactive ^{125}I particles is a form of radiation therapy in which these particles are implanted into tumors or surrounding tissues infiltrated by cancer cells, guided by imaging modalities such as computed tomography (CT) and positron emission tomography-computed tomography (PET-CT) (2). This technique is considered one of the emerging treatment modalities in oncologic radiotherapy. Radioactive ^{125}I particles are directly implanted at the lesion site, where they continuously emit beta particles and gamma rays during their radioactive decay, disrupting the DNA structure of tumor cells and achieving precise targeted therapy (3). A study by Wang *et al* (4) demonstrated that CT-guided close-range radiotherapy with radioactive ^{125}I particles for locally advanced non-small cell lung cancer, following first-line chemotherapy failure, yielded favorable local control rates, effectively alleviating symptoms and improving patients' quality of life. Additionally, research by Ji *et al* (5) confirmed that CT-guided ^{125}I seed implantation is both effective and safe for treating recurrent and/or metastatic malignant tumors in the chest.

Radiation-induced pneumonia (RP) is a common complication associated with radiotherapy. When surrounding normal tissues are exposed to close-range radiation from ^{125}I particles, damage can occur to type II alveolar cells, leading to alveolar collapse and atelectasis, Additionally, endothelial cell damage can result in altered pulmonary blood flow, increased vascular permeability, and capillary obstruction (6). Cytokines such as Interleukin-1 alpha, Tumor Necrosis Factor-alpha (TNF-α) and TNF-β also play a role in the inflammatory response (7). Pathological examinations revealed changes such as alveolar septal edema, endothelial cell swelling and thickening of the vessel wall. Typical clinical symptoms of RP include dyspnea, dry cough, hypoxemia and low-grade fever (8). There is no specific time interval for the onset of RP following close-range radiotherapy. Acute RP typically occurs 4-12 weeks after treatment, while symptoms of delayed or fibrotic RP may appear 6-12 months later. The severity of inflammation is influenced by the volume and dose of radiation received by surrounding normal tissues (9). Currently, various predictive models have been proposed to assess the risk of RP; however, most of these models are based on singular or limited variables and often fail to comprehensively consider individual patient characteristics and biological mechanisms. Due to the complexity and multifactorial nature of RP, there is no definitive model that accurately predicts its occurrence following close-range radiotherapy with radioactive ^{125}I particles. The present study aimed to combine relevant data, including basic patient information, clinical symptoms, tumor characteristics, preoperative laboratory tests, intraoperative data and dose-related parameters of close-range radiotherapy, to predict RP and validate the effectiveness of the model.

A nomogram is a visual statistical tool used to integrate the effects of multiple predictors into a simple and understandable graphic, assisting clinicians in assessing the risk of a specific disease or complication. By assigning a score to each variable, a nomogram allows users to calculate the probability of a particular event (such as the occurrence of RP) based on the patient's specific characteristics.

In medicine, the application of nomograms is becoming increasingly widespread, as they can transform complex multivariable models into intuitive and convenient tools, enhancing the efficiency of clinical decision-making. The present study employed a nomogram to develop a risk prediction model for RP that incorporates multiple relevant variables, thereby providing reliable risk assessment and decision support for clinical practice.

Materials and methods

Study population. The present study included data from 436 patients with advanced lung cancer who underwent close-range radiotherapy with radioactive ^{125}I particles at General Hospital of Northern Theater Command from January 2016 to December 2023 (Shenyang, China). The patients were randomly assigned in a 7:3 ratio, with 305 patients allocated to the modeling cohort and 131 patients included in the internal validation cohort. The inclusion criteria were as follows: i) Poor cardiopulmonary function or advanced age preventing surgical intervention; ii) refusal of surgical intervention; iii) ineligibility for repeat surgery due to postoperative recurrence; iv) patients with residual or progressive tumors after radiotherapy or chemotherapy; v) patients with disease progression following other anti-tumor treatments; and vi) an expected survival of at least 3 months. The exclusion criteria were as follows: i) Poor control of obstructive RP around the lesion, skin infection, or ulceration at the puncture site; ii) patients with severe bleeding tendencies, a platelet count $<50x10^9$/l, or severe coagulation disorders. Anticoagulant therapy and/or platelet medications should be discontinued for at least 5-7 days prior to particle implantation; iii) patients with severe hepatic, renal, cardiac, pulmonary, or cerebral dysfunction, severe anemia, dehydration, and severe nutritional metabolism disturbances that cannot be corrected or improved in the short term, as well as those with severe systemic infections or high fever. All patients included in the present study provided signed informed consent prior to the procedure. The present study was approved (approval no. YL2021-07) by the Ethics Review Committee of the General Hospital of Northern Theater Command in China (Shenyang, China).

Data collection. The present study collected a comprehensive set of perioperative data, including patients' basic information, clinical symptoms, tumor characteristics and preoperative laboratory test results. Patient baseline information comprised: Age, sex, smoking status, Zymosan-Activated Serum (ZPS) scale, key performance indicator system (KPS) score and Numeric Rating Scale (NRS) score. Clinical symptoms include cough, sputum production, chest tightness and shortness of breath. Tumor characteristics encompassed: Preoperative lung cancer diameter, preoperative TNM staging, tumor location, preoperative lung atelectasis, obstructive pneumonia, superior vena cava obstruction syndrome. Preoperative laboratory tests included: Carcinoembryonic antigen (CEA), neuron-specific enolase (Nse), cytokeratin 19 fragment, squamous cell carcinoma (SCC) antigen, and preoperative white blood cell count. Additionally, intraoperative data and dosimetric parameters related to close-range radiotherapy dose were collected: Surgical time, planned target volume (PTV), maximum dose, average dose, single particle dose, preoperative diameter at 90% cumulative volume (D_{90}) and volume at 100% cumulative volume (V_{100}), D_{90} and V_{100} of the 1-cm and 2-cm irradiated areas around the lesion (represented as $X_{1\ cm}D_{90}$, $X_{2\ cm}D_{90}$, $X_{1\ cm}V_{100}$, $X_{2\ cm}V_{100}$), number of particles, puncture needle path and puncture distance.

Close-range radiotherapy method using radioactive ^{125}I particles. Preoperative planning: Imaging studies (CT, enhanced CT, PET-CT) are transferred to a three-dimensional treatment planning system. Treatment plans are designed within this system, establishing pre-treatment protocols that determine the number of implanted needles, their positions, and the number and placement of particles. Individual particle activities are selected, total activity in the target area is calculated, and the anticipated dose distribution in both tumor and normal tissues. Intraoperative procedure: Based on the patient's condition, an appropriate position was chosen and was secured. Local anesthesia is administered for the implantation of radioactive particles. The implantation is performed under CT guidance, with a routine scan of 0.5-cm slice thickness to local the tumor and mark the corresponding range

on the body surface. According to the TPS treatment plan, the appropriate intercostal space is selected as the puncture implantation plane, and the needle insertion position, angle and depth are determined. Under CT guidance, the particle needle is inserted into the predetermined position within the tumor, and particles are implanted according to the TPS plan. The particle needle is inserted in a single motion to minimize the dose received by the operator during implantation and to reduce the risk of postoperative pneumothorax. A pen-style implantation gun is used to implant the particles in a retractable manner, with spacing of 0.5-1.5 cm between particles. During the procedure, the patient's heart rate, blood pressure and blood oxygen saturation are continuously monitored. The patient's level of consciousness, breathing, pain, coughing, and any hemoptysis are also observed and symptomatic treatment is provided as needed. Following particle implantation, postoperative CT images are uploaded into the TPS for quality assessment, focusing on particle and dose reconstruction. After the procedure, the patient is monitored with electrocardiogram and oxygen therapy until their condition stabilizes. A follow-up chest CT scan is conducted 24 h postoperatively to check for any secondary pneumothorax, hemothorax, or particle displacement.

The grading of radiation pneumonitis and symptomatic treatment. Radiation pneumonitis refers to a series of pathological and physiological changes induced by the irradiation of a certain volume of normal lung tissue by particles. This condition can lead to acute exudative or tissue fibrotic changes, ultimately impairing the patient's respiratory function. Grade 0: No abnormalities. Grade 1: Mild dry cough or shortness of breath after exertion. Grade 2: Persistent cough requiring antitussive medication and mild exertional dyspnea with no dyspnea at rest. Symptomatic support and antibiotics (consider corticosteroids) are required for fever, acute exudative changes on chest CT, or elevated neutrophil percentage require. Grade 3: Severe cough that is unresponsive to antitussive medication, or dyspnea at rest. Intermittent oxygen therapy is necessary if there is clinical or radiographic evidence of acute pneumonia, and steroid therapy may be required. Grade 4: Severe respiratory failure necessitating continuous oxygen therapy and mechanical ventilation.

Statistical analysis. R software (Version 4.1.2; https://www.R-project.org) was utilized for statistical analysis, while Graphpad Prism (Version 6.0; Dotmatics) was employed to create forest plots. The data were randomly divided into a training set and a validation set in a 7:3 ratio. All data were assessed for normality using the Kolmogorov-Smirnov test. For continuous variables with normal distribution, the mean and standard deviation were calculated, and unpaired Student's t test was applied. The Mann-Whitney U test was employed to evaluate non-normally distributed data, which are expressed as the median (interquartile range). Comparative analysis of categorical variables was performed using Pearson chi-square test or Fisher's exact test, with results presented as P-values and percentages. Subsequently, the least absolute shrinkage and selection operator (LASSO) method was applied to identify potential predictive features. Multivariable logistic regression analysis was conducted on variables with P<0.05 from the univariate analysis. And a line chart prediction model for radiation pneumonitis due to late-stage lung cancer treated with radioactive ^{125}I particle brachytherapy was developed using the four selected variables. A calibration curve was plotted to assess the calibration of the line chart and the discriminatory performance was measured using receiver operating characteristic (ROC) curve. The clinical utility of the line chart was evaluated through decision curve analysis (DCA) by measuring the net benefit at different probability thresholds. The incidence rates of RP at different grades were estimated using the Kaplan-Meier method, and differences in RP incidence rates between groups were compared using the log-rank test. The flowchart detailing these procedures is presented in Fig. 1.

Results

The baseline data. The present study included 436 patients with late-stage lung cancer who underwent radioactive ^{125}I particle brachytherapy. The patients were randomly allocated in a 7:3 ratio, with 305 patients assigned to the modeling cohort and 131 patients included in the internal validation cohort. The modeling cohort consisted of 134 men with a mean age of 62.37±10.37 years, while the internal validation cohort included 67 males with a mean age of 64.29±10.35 years. Statistical analysis was performed on patient demographics, clinical symptoms, general tumor characteristics, and preoperative laboratory tests in the both cohorts. These variables included: Age, sex, smoking status, ZPS scale, KPS score, NRS score, clinical symptoms (cough, sputum, chest tightness, dyspnea), preoperative lung cancer diameter, preoperative TNM staging, tumor location, preoperative lung collapse, obstructive pneumonia, superior vena cava obstruction syndrome and laboratory test results (preoperative CEA, preoperative Nse, preoperative cytokeratin 19 fragment, preoperative SCC and white blood cell count). In addition, intraoperative data and relevant dosimetric parameters for brachytherapy were collected, including: operation time, PTV volume, maximum dose, average dose, single particle dose, preoperative D_{90} and V_{100}, $X_{1\ cm}D_{90}$, $X_{2\ cm}D_{90}$, $X_{1\ cm}V_{100}$, $X_{2\ cm}V_{100}$, number of particles, puncture needle path and puncture distance. There were no significant statistical differences in any of these data between the two cohorts (all P>0.05, Table I).

Factors influencing RP following brachytherapy for late-stage lung cancer. Based on LASSO Logistic regression, the independent variables in the dataset were screened, and those corresponding to non-zero coefficients at Lambda.min were selected for subsequent multivariate analysis. As illustrated in Fig. 2, the selected variables include: Smoking status, preoperative N and M staging, superior vena cava obstruction syndrome, preoperative white blood cells, maximum dose and chemotherapy. To further evaluate seven potential predictive factors and optimize the predictive model, a multivariable logistic regression analysis was conducted. The results indicated that preoperative N_3 stage [95% CI, 2.171 (1.234-3.821), P=0.007], preoperative M_1 stage [95% CI, 2,955 (1.667-5.237), P<0.001], maximum dose [95% CI 1.000, (1.000-1.000), P=0.002] and chemotherapy [95% CI, 0.586 (0.343-1.002), P=0.049] were independent risk factors influencing RP in

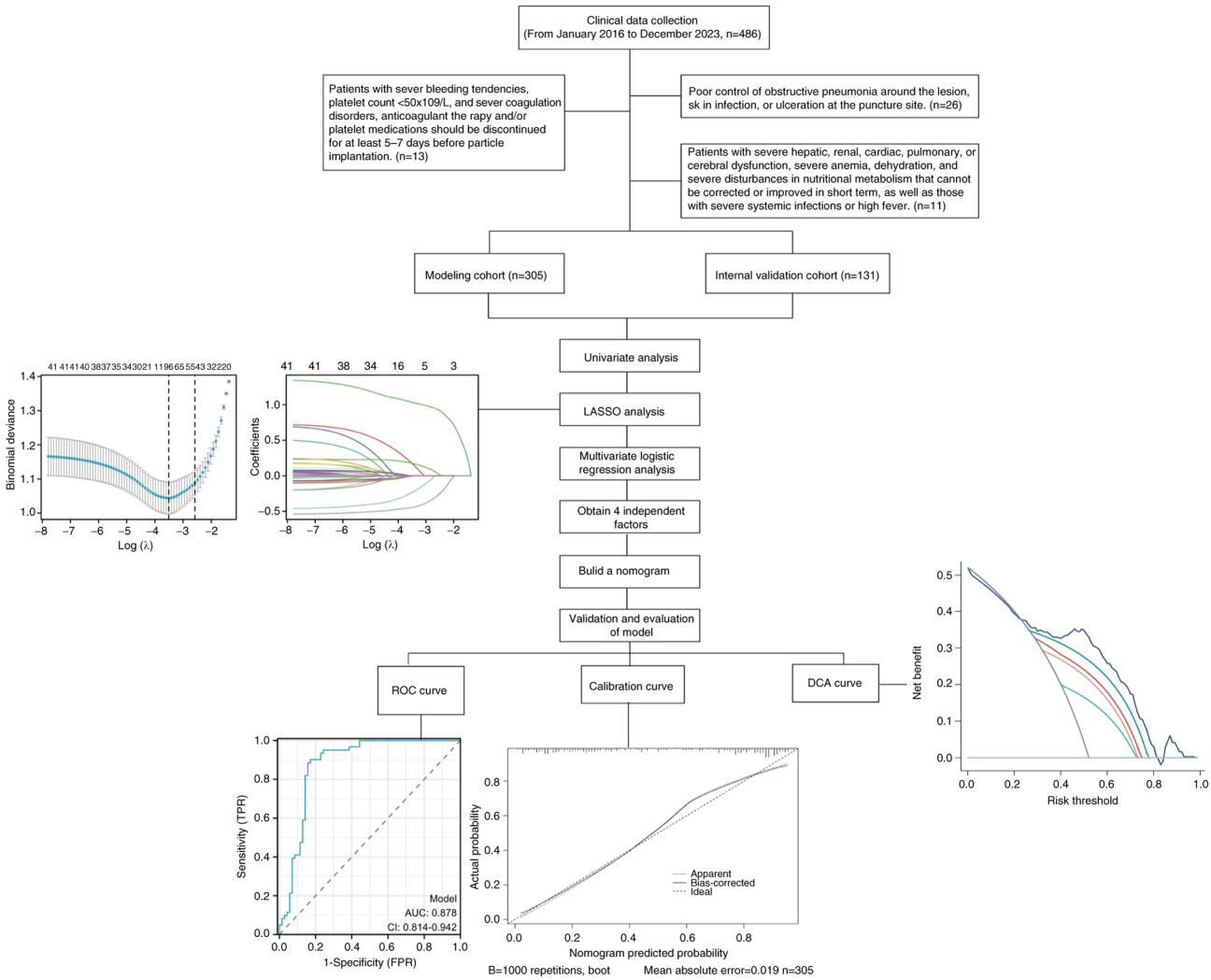

Figure 1. Flowchart. LASSO, least absolute shrinkage and selection operator; ROC, receiver operating characteristic; DCA, decision curve analysis.

patients with late-stage lung cancer treated with brachytherapy, as summarized in Table II and depicted in Fig. 3.

Development and validation of the predictive model. A nomogram plot (Fig. 4) was constructed based on four independent risk factors: Preoperative N and M staging, maximum dose and whether chemotherapy was administered. To use the nomogram, a vertical line is drawn for each variable to determine its respective score. By summing those scores, the total score, which indicates the risk probability of RP, can be calculated. For example, a patient with a preoperative $T_3N_2M_1$ stage, a maximum dose of 136510 Gy, and who received preoperative chemotherapy would have a total score of 114 points, corresponding to a 77% risk of RP.

As illustrated in Fig. 5, the area under the ROC curve in the training set (Fig. 5A) was 0.878 (95% CI, 0.814-0.942). The calibration curve and ROC curve for the validation set yielded results similar to those in the training set, with the area under the ROC curve in the validation set (Fig. 5B) being 0.828 (95% CI, 0.787-0.870). For individual predictors in the training set (Fig. 5C), the area under the ROC curve was 0.778 (95% CI, 0.706-0.850) for smoking, 0.751 (95% CI, 0.674-0.828) for preoperative N staging, 0.794 (95% CI, 0.725-0.864) for preoperative M staging, 0.874 (95% CI, 0.808-0.940) for maximum dose, and 0.805 (95% CI, 0.737-0.872) for preoperative chemotherapy. In the validation set (Fig. 5D), the areas under the ROC curve were 0.650 (95% CI, 0.607-0.693) for smoking, 0.713 (95% CI, 0.669-0.758) for preoperative N staging, 0.755 (95% CI, 0.715-0.795) for preoperative M staging, 0.832 (95% CI, 0.791-0.873) for maximum dose, and 0.705 (95% CI, 0.662-0.748) for preoperative chemotherapy. The calibration curves indicate that both the training (Fig. 5E) and validation (Fig. 5F) set were close to the 45-degree line, indicating that the model accurately predicts actual events.

DCA demonstrates that clinical decisions based on the predictive model are beneficial, highlighting the practical clinical application and feasibility of the model in both the training set (Fig. 6A) and validation set (Fig. 6B). Among the variables, maximum dose achieves the most significant clinical benefits in practice, showing promising prospects for clinical application. The maximum dose provides the highest benefits in both the training and validation sets (Fig. 6C and D).

Grading of RP and Kaplan-Meier analysis. Based on the grading of RP, the data were divided into two RP of grade 2 or below and grade 3 or higher. In the group with RP of grade 3

Table I. Baseline data.

Variable	Total (n=436)	train_set (n=305)	valid_set (n=131)	Statistic	P-value
Year, Mean ± SD	62.95±10.39	62.37±10.37	64.29±10.35	t=-1.773	0.077
Preoperative longitudinal diameter, Mean ± SD	4.49±1.08	4.51±1.10	4.44±1.04	t=0.565	0.572
Zubrod ECOG WHO Performance Status zymosan-activated serum scale five-point scale, Mean ± SD	2.05±0.78	2.05±0.77	2.05±0.80	t=-0.093	0.926
Karnofsky Performance Status key performance indicator system score, Mean ± SD	76.06±10.57	75.90±10.63	76.41±10.46	t=-0.462	0.644
Numeric Rating Scale score, Mean ± SD	3.89±1.53	3.90±1.59	3.84±1.37	t=0.434	0.665
Preoperative carcinoembryonic antigen, Mean ± SD	5.15±4.40	5.21±4.82	5.02±3.26	t=0.410	0.682
Preoperative neuron specific enolase, Mean ± SD	10.98±10.19	10.78±9.76	11.42±11.16	t=-0.602	0.547
Preoperative cytokeratin 19 fragment, Mean ± SD	5.64±6.16	5.95±6.37	4.92±5.59	t=1.615	0.107
Preoperative squamous cell carcinoma antigen, Mean ± SD	3.97±3.12	3.99±3.03	3.91±3.33	t=0.248	0.804
Preoperative white blood cells, Mean ± SD	6.14±2.20	6.11±2.27	6.20±2.04	t=-0.377	0.707
Planning target volume, Mean ± SD	14.82±7.26	14.71±7.31	15.05±7.17	t=-0.450	0.653
Maximum dose, Mean ± SD	141016.46±42196.25	143900.33±40194.77	134302.10±45988.02	t=2.187	0.059
Mean dose, Mean ± SD	43000.70±5607.01	42755.98±5823.37	43570.47±5042.76	t=-1.392	0.165
Preoperative D90, Mean ± SD	16059.98±3333.95	16068.28±3314.52	16040.66±3391.49	t=0.079	0.937
Preoperativev100, Mean ± SD	94.08±1.45	94.01±1.43	94.24±1.47	t=-1.507	0.133
$X_{1\ cm}$D90, Mean ± SD	12228.99± 2622.87	12160.97± 2663.68	12387.36± 2528.21	t=-0.826	0.409
$X_{1\ cm}$V100, Mean ± SD	93.49±1.85	93.44 ± 1.84	93.62 ± 1.87	t=-0.952	0.342
$X_{2\ cm}$D90, Mean ± SD	9624.29±1755.06	9628.42±1799.53	9614.66±1653.52	t=0.075	0.940
$X_{2\ cm}$V100, Mean ± SD	91.26±2.29	91.28±2.38	91.22±2.08	t=0.227	0.821
Number of implanted particles, Mean ± SD	82.15±25.62	81.66±26.00	83.27±24.77	t=-0.602	0.547
Surgical duration, Mean ± SD	47.55±11.86	47.16±11.74	48.46±12.14	t=-1.050	0.294
Puncture needle tract, Mean ± SD	14.15±7.63	14.13±7.78	14.19±7.29	t=-0.079	0.937
Puncture distance, Mean ± SD	0.68±0.35	0.68±0.36	0.66±0.35	t=0.622	0.534
Sex, n (%)				χ^2=1.918	0.166
Male	201 (46.1)	134 (43.93)	67 (51.15)		
Female	235 (53.9)	171 (56.07)	64 (48.85)		
Smoke, n (%)				χ^2=0.779	0.377
Yes	160 (36.7)	116 (38.03)	44 (33.59)		
No	276 (63.3)	189 (61.97)	87 (66.41)		
Primary tumor pathology type, n (%)				-	0.445
Adenocarcinoma of the lung	217 (49.77)	157 (51.48)	60 (45.80)		
Squamous cell carcinoma of the lung	111 (25.46)	74 (24.26)	37 (28.24)		

Table I. Continued.

Variable	Total (n=436)	train_set (n=305)	valid_set (n=131)	Statistic	P-value
Small cell lung cancer	98 (22.48)	69 (22.62)	29 (22.14)		
Neuroendocrine tumor	5 (1.15)	2 (0.66)	3 (2.29)		
Cancer with SMARCA4 deficiency	5 (1.15)	3 (0.98)	2 (1.53)		
Preoperative T, n (%)				χ^2=2.983	0.225
2	144 (33.03)	93 (30.49)	51 (38.93)		
3	180 (41.28)	130 (42.62)	50 (38.17)		
4	112 (25.69)	82 (26.89)	30 (22.90)		
Preoperative N, n (%)				χ^2=5.531	0.063
1	35 (8.03)	24 (7.87)	11 (8.40)		
2	188 (43.12)	121 (39.67)	67 (51.15)		
3	213 (48.85)	160 (52.46)	53 (40.46)		
Preoperative M, n (%)				χ^2=0.011	0.917
0	218 (50)	153 (50.16)	65 (49.62)		
1	218 (50)	152 (49.84)	66 (50.38)		
Pulmonary lobe, n (%)				χ^2=1.005	0.316
Left lung	298 (68.35)	204 (66.89)	94 (71.76)		
Right lung	138 (31.65)	101 (33.11)	37 (28.24)		
Pulmonary segment, n (%)				χ^2=1.258	0.533
Upper lobe of the lung	157 (36.01)	109 (35.74)	48 (36.64)		
Middle lobe of the lung	44 (10.09)	34 (11.15)	10 (7.63)		
Lower lobe of the lung	235 (53.9)	162 (53.11)	73 (55.73)		
Atelectasis, n (%)				χ^2=0.150	0.699
Yes	177 (40.6)	122 (40.00)	55 (41.98)		
No	259 (59.4)	183 (60.00)	76 (58.02)		
Obstructive pneumonia, n (%)				χ^2=0.053	0.819
Yes	210 (48.17)	148 (48.52)	62 (47.33)		
No	226 (51.83)	157 (51.48)	69 (52.67)		
Superior vena cava obstruction, n (%)				χ^2=2.141	0.143
Yes	213 (48.85)	142 (46.56)	71 (54.20)		
No	223 (51.15)	163 (53.44)	60 (45.80)		
Cough, n (%)				χ^2=0.022	0.881
Yes	194 (44.5)	135 (44.26)	59 (45.04)		
No	242 (55.5)	170 (55.74)	72 (54.96)		

Table I. Continued.

Variable	Total (n=436)	train_set (n=305)	valid_set (n=131)	Statistic	P-value
Expectoration, n (%)				χ^2=0.475	0.491
Yes	214 (49.08)	153 (50.16)	61 (46.56)		
No	222 (50.92)	152 (49.84)	70 (53.44)		
Chest tightness and shortness of breath, n (%)				χ^2=2.391	0.122
Yes	211 (48.39)	155 (50.82)	56 (42.75)		
No	225 (51.61)	150 (49.18)	75 (57.25)		
Asthma, n (%)				χ^2=0.158	0.691
Yes	210 (48.17)	145 (47.54)	65 (49.62)		
No	226 (51.83)	160 (52.46)	66 (50.38)		
Particle spacing (mCi), n (%)				χ^2=5.193	0.268
0.5	81 (18.58)	52 (17.05)	29 (22.14)		
0.6	96 (22.02)	75 (24.59)	21 (16.03)		
0.7	66 (15.14)	48 (15.74)	18 (13.74)		
0.9	25 (5.73)	17 (5.57)	8 (6.11)		
1	168 (38.53)	113 (37.05)	55 (41.98)		
Radiotherapy, n (%)				χ^2=1.646	0.199
Yes	196 (44.95)	131 (42.95)	65 (49.62)		
No	240 (55.05)	174 (57.05)	66 (50.38)		
Chemotherapy, n (%)				χ^2=1.418	0.234
Yes	212 (48.62)	154 (50.49)	58 (44.27)		
No	224 (51.38)	151 (49.51)	73 (55.73)		

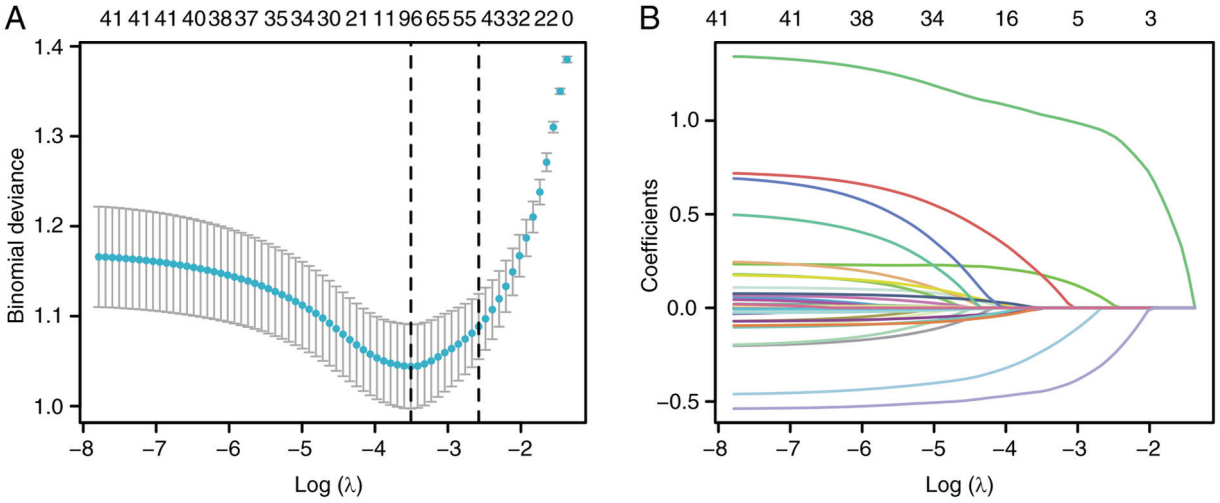

Figure 2. The feature selection using LASSO Logistic regression. (A) Parameter tuning (λ) selection was performed using 10-fold cross-validation in LASSO Logistic regression, and a plot of binomial deviation against log(λ) was created based on the minimum criteria. The black vertical line marks the optimal λ based on both the minimum criteria and minimum standard error. (B) LASSO coefficient profiles of 10 clinical factors. A plot of coefficient profiles corresponding to log(λ) is demonstrated. LASSO, least absolute shrinkage and selection operator.

or higher, the average maximum dose is 139,187.27 mCi, while in the group with grade 2 or below, it is 129,864.09 mCi.

Patients with preoperative T1 and T3 staging (P<0.001) (Fig. 7A), preoperative M1 staging [P<0.01, HR=8.26 (4.66-14.64)] (Fig. 7C), a maximum dose exceeding 139,187.27 mCi [P<0.001, HR=9.63 (4.61-20.12)] (Fig. 7E), and those who underwent preoperative chemotherapy [P<0.001, HR=0.12 (0.07-0.22)] (Fig. 7G) were found to be more likely to develop RP of grade 3 or higher (P<0.001). Specifically, for patients with T3 staging, the probability of developing pneumonia of grade 3 or higher at 6 and 12 weeks was 15 and 24%, respectively. For patients with M1 staging developing pneumonia of grade 3 or higher at 6 weeks and 12 weeks is 12 and 29%, respectively. Patients who underwent chemotherapy have a 10% probability at 6 weeks and 22% probability at 12 weeks of developing pneumonia of grade 3 or higher.

Conversely, for RP of grade 2 or lower, patients with preoperative T1 and T3 staging (P<0.001) (Fig. 7B), preoperative M1 staging [P<0.01, HR=4.64 (3.36-6.41)] (Fig. 7D), and a maximum dose exceeding 139,187.27 mCi [P<0.001, HR=8.46 (5.79-12.35)] (Fig. 7F), and those who underwent preoperative chemotherapy [P<0.001, HR=0.33 (0.25-0.44)] (Fig. 7H) were found to be more likely to develop RP of grade 2 or below (P<0.001). Specifically, for patients with T3 staging, the probability of developing pneumonia of grade 2 or below at 6 and 12 weeks was 20 and 41%, respectively. For patients with M1 staging, these probabilities were 18% at 6 weeks and 33% at 12 weeks. Patients who underwent chemotherapy had an 18% probability at 6 weeks and 36% probability at 12 weeks of developing pneumonia of grade 2 or below.

Discussion

In 2022, lung cancer ranked first among all new cases of malignant tumors in China, accounting for 18.06% of the total cancer cases. Similarly, lung cancer accounted for 23.9% of all deaths from malignant tumors in China, also ranking first (10). Early-stage lung cancer often presents with no obvious symptoms, and in clinical practice, most patients seek medical attention when symptoms appear, by which time it is already in the advanced stage, leading to a loss of the opportunity for surgery. The overall 5-year survival rate for patients with advanced-stage lung cancer is ~15% (11). Radioactive ^{125}I particle brachytherapy, radio-chemotherapy and targeted immunotherapy techniques are widely used in the treatment of advanced lung cancer (12). The radioactive ^{125}I particle brachytherapy has the advantages of minimal complications and significant efficacy, leading to a rapid increase in the number of patients with advanced lung cancer receiving this treatment annually. In epidermal growth factor receptor tyrosine kinase inhibitor treatment failure, 58.6% of patients experience progression of the original lesion, while 20.7% of patients have both progression of the original lesion and the emergence of new lesions. Therefore, radioactive ^{125}I particle brachytherapy can effectively provide local control of the original lesion, thereby extending the patients' progression-free survival and overall survival (OS) (13). A study by Zhang *et al* (14) reported that in patients with oligo-recurrence after first-line chemotherapy failure in non-small cell lung cancer, the short-term efficacy and quality of life of those receiving radioactive ^{125}I particle implantation therapy were superior to those continuing chemotherapy, while the OS was comparable. Compared with external beam radiation therapy, radioactive ^{125}I particle brachytherapy avoids the disadvantage of expanding the irradiation range due to respiratory motion, thereby effectively reducing damage to surrounding normal tissues (15). The incidence of radiation pneumonitis after combined radio chemotherapy for non-small cell lung cancer is 43.33%, while the incidence of radiation pneumonitis with radioactive ^{125}I particle implantation therapy is 6.25%. Both approaches have similar short-term efficacy rates and 1 and 2-year OS rates (16). Brachytherapy is particularly effective in treating certain types of tumors, but it still faces numerous challenges in predicting and managing RP, which underscores the significance of the present study. Uneven dose distribution: Brachytherapy typically uses high-dose rate or low-dose rate

Table II. Logistic univariate and multivariate regression analysis of risk factors for radiation pneumonia following brachytherapy for late-stage lung cancer.

		Univariate analysis		Multivariate analysis	
Characteristics	Total (N)	Odds ratio (95% CI)	P-value	Odds ratio (95% CI)	P-value
Smoke	436				
No	276	Reference		Reference	
Yes	160	3.919 (2.569-5.978)	<0.001	1.598 (0.944-2.707)	0.081
Preoperative N	436				
1	35	Reference		Reference	
2	188	1.654 (0.784-3.490)	0.186	1.998 (0.854 4.673)	0.111
3	213	7.307 (4.698-11.364)	<0.001	2.171 (1.234-3.821)	0.007
Preoperative M	436				
0	218	Reference		Reference	
1	218	9.514 (6.143-14.736)	<0.001	2.955 (1.667-5.237)	<0.001
preoperative white blood cells	436	0.942 (0.864-1.027)	0.177		
Maximum dose	436	1.000 (1.000-1.000)	<0.001	1.000 (1.000-1.000)	0.002
Chemotherapy	436				
Yes	212	Reference		Reference	
No	224	0.174 (0.115-0.263)	<0.001	0.586 (0.343-1.002)	0.049
Superior vena cava obstruction	436				
Yes	213	Reference			
No	223	1.388 (0.952-2.024)	0.088		0.091

CI, confidence interval.

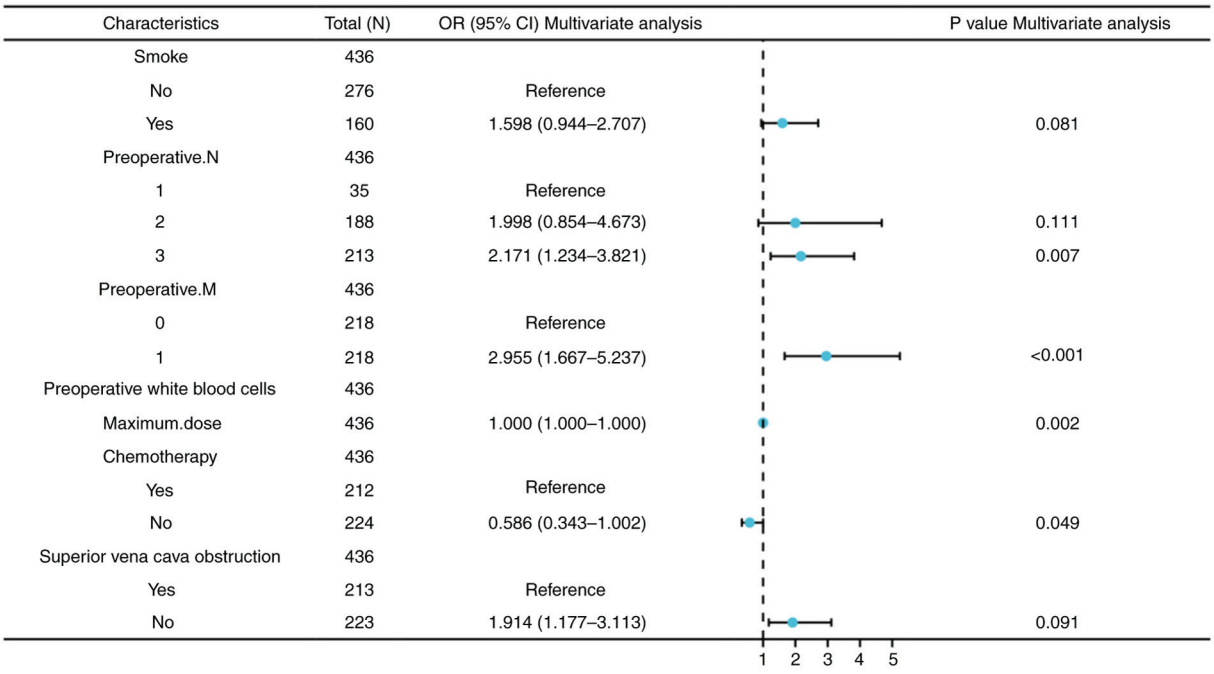

Figure 3. Forest plot of multivariable logistic regression analysis of radiation pneumonia following brachytherapy for late-stage lung cancer. OR, odds ratio; CI, confidence interval.

radiation sources, resulting in complex dose distributions that may lead to some healthy lung tissue receiving excessively high radiation doses. This heterogeneity in dosing complicates risk assessment, as different patients and treatment protocols can lead to variable dose exposures. Biological heterogeneity: There may be significant differences in the biological

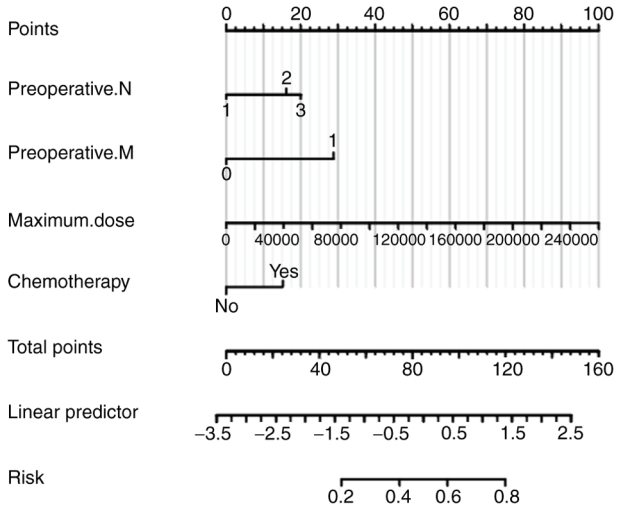

Figure 4. A nomogram for predicting radiation pneumonia following stereotactic radiotherapy for advanced lung cancer. A nomogram was constructed using logistic multivariate regression, including preoperative N staging, preoperative M staging, maximum dose, and whether chemotherapy was administered.

characteristics of lung tissue among patients, including lung function, tissue response and individual sensitivity to radiation. This heterogeneity makes predictions based on a single marker or risk factor less accurate, increasing the complexity of managing RP. Complexity of clinical assessment: The symptoms of RP can be similar to those of other complications (such as infections or tumor progression), making it challenging for clinicians to recognize and diagnose RP early on. This misdiagnosis or late diagnosis may adversely affect patient management and treatment outcomes. Lack of standardized predictive models: Currently, while there are some risk assessment tools available, there are still limited standardized predictive models that specifically address the unique risk factors associated with brachytherapy. This results in a lack of effective tools in clinical practice to predict and manage the risk of RP, thereby limiting the implementation of personalized treatment. The significance of the present study lies in filling these gaps by developing a predictive model that can more accurately identify RP risk factors associated with brachytherapy and providing clinicians with practical management strategies. In doing so, it was aimed to enhance the accuracy of RP predictions, deliver improved treatment outcomes for patients, and improve their quality of life.

The present study collected data from 436 patients with advanced lung cancer who underwent radioactive ^{125}I particle brachytherapy. These patients were randomly assigned in a 7:3 ratio, with 305 patients allocated to the modeling cohort and 131 patients included in the internal validation cohort. Since the research was conducted in a military hospital, collaboration with other medical institutions poses certain challenges. In the future, the authors plan to gradually initiate collaborative projects with local hospitals to expand their sample size, thereby improving the statistical accuracy. Currently in the present study, combining patient demographics, clinical symptoms, tumor characteristics, preoperative laboratory tests, intraoperative data and brachytherapy dosage for screening, LASSO logistic variable selection identified non-zero coefficient variables including: Smoking, preoperative N and M staging, superior vena cava syndrome, preoperative white blood cell count, maximum dose and chemotherapy. Further evaluation using a multiple logistic regression model revealed that preoperative N_3 stage [95% CI, 2.171 (1.234-3.821), P=0.007], preoperative M_1 stage [95% CI, 2.955 (1.667-5.237), P<0.001], maximum dose (95% CI, 1.000 (1.000-1.000), P=0.002) and chemotherapy [95% CI, 0.586 (0.343-1.002), P=0.049] were independent risk factors influencing radiation pneumonitis in patients with advanced lung cancer undergoing brachytherapy. The correlation between tumor volume, tumor staging and radiation pneumonitis is controversial.

Some studies suggest that higher tumor TNM staging, larger volume, closer proximity to the hilum or lower lung, and a larger irradiated lung volume are associated with an increased risk of radiation pneumonitis. This is consistent with the findings of De Petris *et al* (17). However, other studies have revealed that tumor volume is not related to the occurrence of radiation pneumonitis (18). This is mainly related to other confounding factors such as patient lung volume size and volume of lung tissue irradiated (19). When combined radiotherapy is used, it leads to exudative and inflammatory changes in the local lung tissue, a reduction in type II alveolar cells and surfactant, and a series of pathophysiological changes in the blood vessel wall and lung tissue. The combined toxic effects exacerbate lung damage, making radiation pneumonitis more likely to occur and difficult to recover from when combined with chemotherapy. The study by Zha *et al* (16) confirmed that chemotherapy is an important factor in accurately predicting symptomatic pneumonitis. Together with age, smoking index and whole lung volume at 5 Gy/mean lung dose, they constructed a nomogram prediction model with an area under the ROC curve of 0.89, demonstrating favorable calibration. Chemotherapy, as a significant risk factor for predicting radiation pneumonitis, is consistent with the results of the aforementioned study. The authors understand the potential value of conducting stratified analyses based on different chemotherapy regimens or timing (for example, combination therapy vs. sequential therapy), as this could indeed provide more specific guidance for clinical decision-making. However, due to the sample size of the present study and the availability of data, categorizing chemotherapy regimens and timing at this stage may lead to instability in the statistical results and complexity in interpretation. Therefore, stratified analyses were decided not to be performed on chemotherapy regimens and timing in order to maintain the rigor of the present study and the reliability of the results. This direction will be considered in future research.

There is still controversy regarding the correlation between dosimetric parameters and the occurrence of radiation pneumonitis. The study by Bi *et al* (20) concluded that the MLD is the most critical dose-volume parameter influencing radiation pneumonitis, and it can improve prevention of the occurrence of radiation pneumonitis in patients undergoing combined immunotherapy and radiotherapy. On the other hand, Ji *et al* (21) hypothesized that there is no clear correlation between dosimetric parameters and the occurrence of postoperative radiation pneumonitis. The correlation between radiotherapy dose and radiation pneumonitis cannot be directly applied to the prediction of radiation pneumonitis in

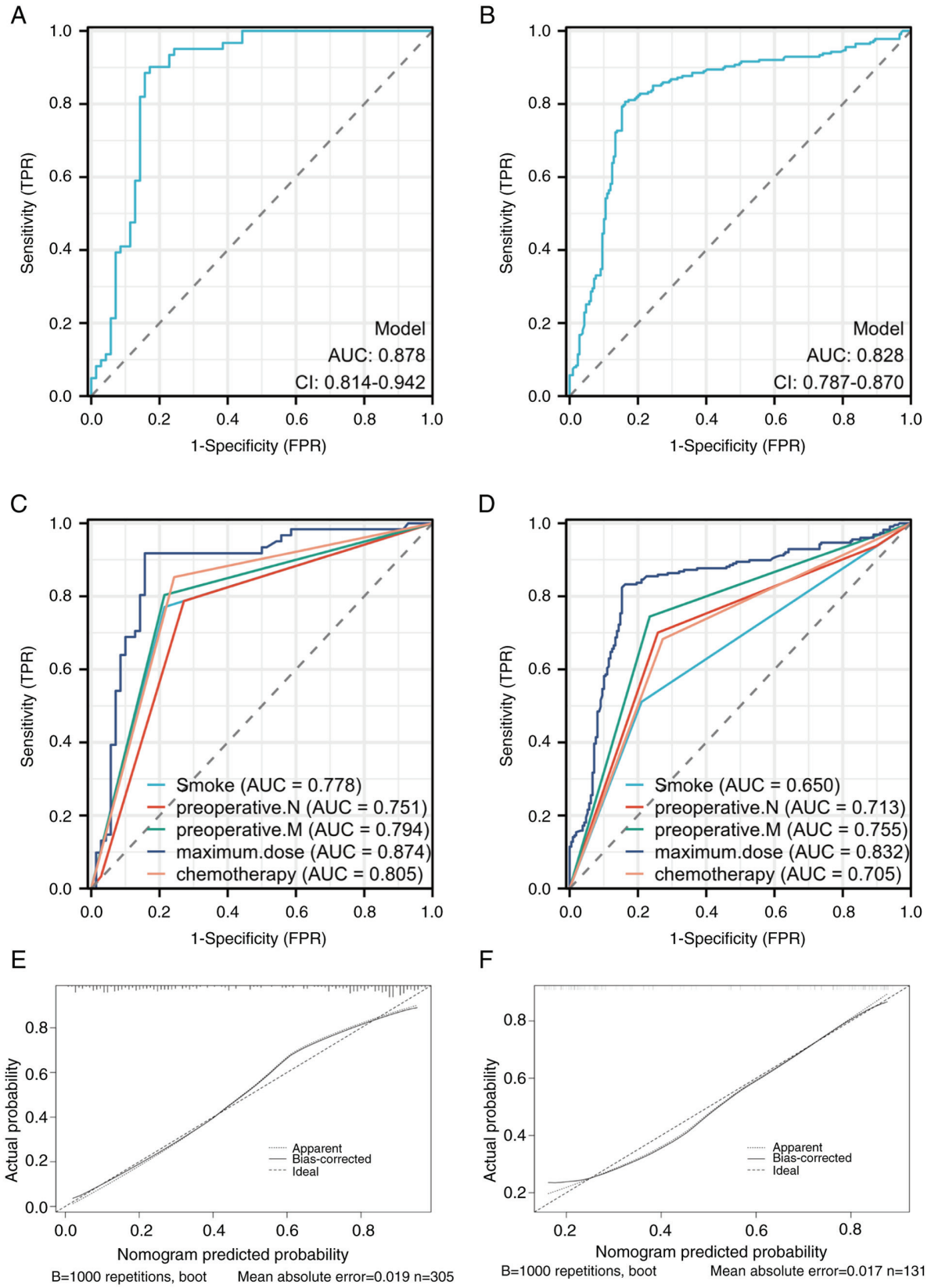

Figure 5. The receiver operating characteristic curves of the prediction model in the (A) training set and (B) validation set are demonstrated. (C) ROC curves for the training set and (D) validation set grouped by Smoke, Preoperative N, Preoperative M, maximum dose and chemotherapy. (E) Calibration curves for the training set and the (F) validation set. AUC, area under curve; CI, confidence interval; FPR, false positive rate; TPR, true positive rate.

brachytherapy using radioactive ^{125}I particles. The conclusion of the present study is that among dosimetric parameters, only the maximum dose is a predictor of radiation pneumonitis, which is consistent with the findings of Flakus *et al* (22). Moreover, it is noteworthy that the maximum dose as a predictor of radiation pneumonitis in brachytherapy with

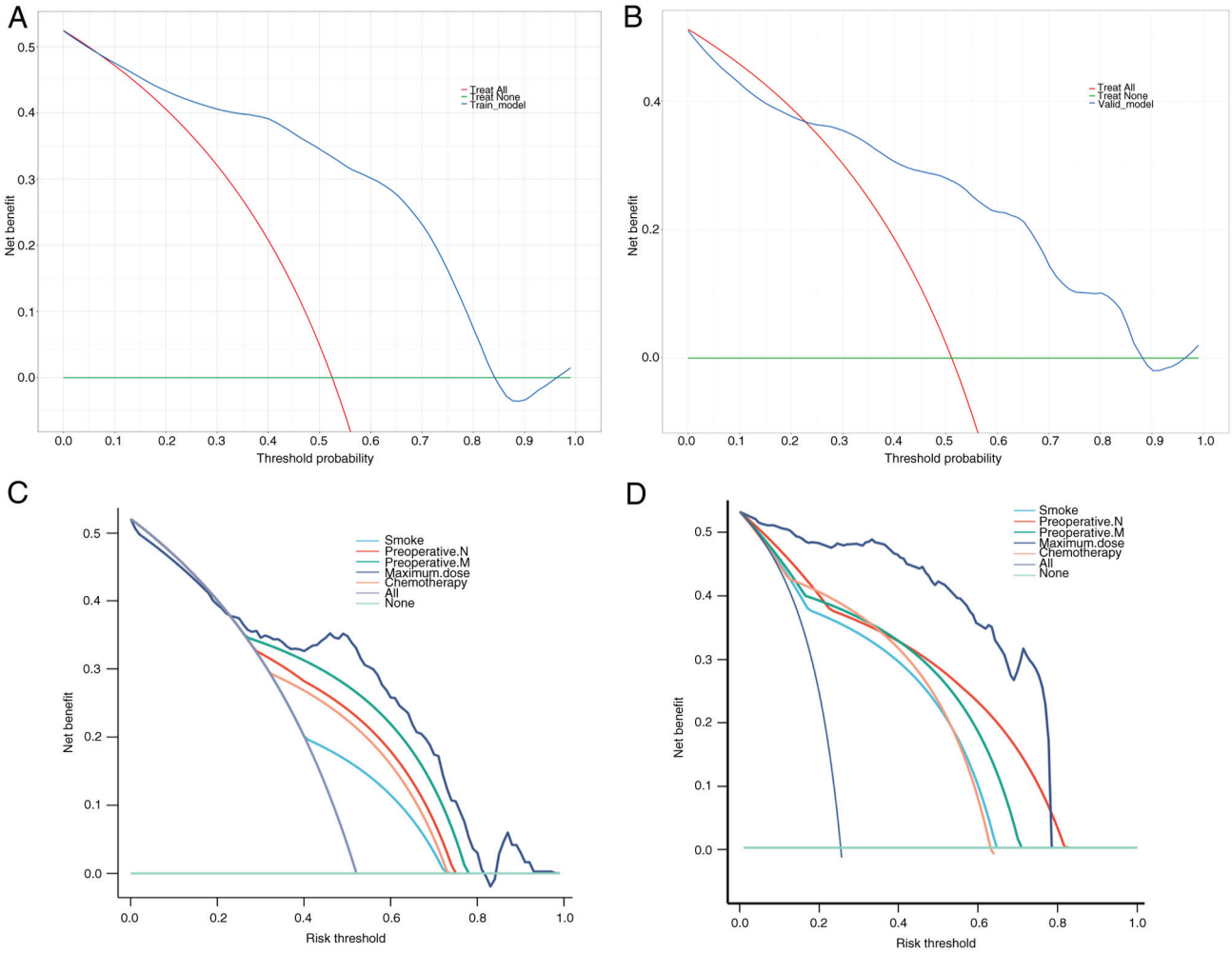

Figure 6. Decision curve analysis. (A) DCA plot for the training set. (B) DCA plot for the validation set. (C) DCA plot for multiple models in the training set. (D) DCA plot for multiple models in the validation set. (C and D) indicate that the maximum dose provides the highest benefit in both the training and validation sets.

radioactive ^{125}I particles is a significant finding that adds to the understanding of the complex relationship between radiotherapy and lung toxicity. While dosimetric parameters may not always correlate directly with the occurrence of radiation pneumonitis, the maximum dose appears to be a critical factor in brachytherapy, possibly due to the localized high-dose delivery characteristics of this treatment modality. Regarding the implications of this finding for treatment planning and dose limitations, reassessment of current dosing standards and treatment protocols may be needed to ensure that the selection of the maximum dose effectively targets the tumor while not excessively increasing the risk of RP. This may involve individualized dose adjustment, assessment of pulmonary sensitivity and a comprehensive application of other therapeutic modalities to mitigate potential side effects.

Furthermore, the present study underscores the need for a comprehensive approach in predicting and managing radiation pneumonitis. Age, smoking history and other patient-specific factors must be considered along with dosimetric parameters to develop accurate prediction models. Additionally, the combined effects of radiotherapy and chemotherapy on lung tissue need to be carefully evaluated to optimize treatment outcomes and minimize toxicity. Time-to-event analysis was considered to be included in the predictive model and the possibility of developing a nomogram to update risk predictions over time as well as creating an online calculator was explored. However, the current understanding of this approach is limited, which prevented the authors from implementing it in the present study. Additionally, it was observed that some relevant literature also did not include dynamic nomograms or online calculators but instead opted for static risk prediction models. Nevertheless, this did not hinder the present study from obtaining valuable predictive results (23).

The predictors identified in the present study primarily emphasize the individual characteristics of patients (such as age, underlying diseases and lung function) as well as the specific characteristics of the tumor (such as N and M classifications). These factors reflect the biological characteristics and treatment suitability of the patients when undergoing radiation therapy, providing a basis for personalized treatment. By contrast, the predictors for EBRT typically place greater emphasis on the radiation dose, irradiated area, radiation technique and specific implementation details of the treatment. These factors directly affect the extent of radiation's impact on lung tissue and are essential components in assessing the risk of RP. By comparing the

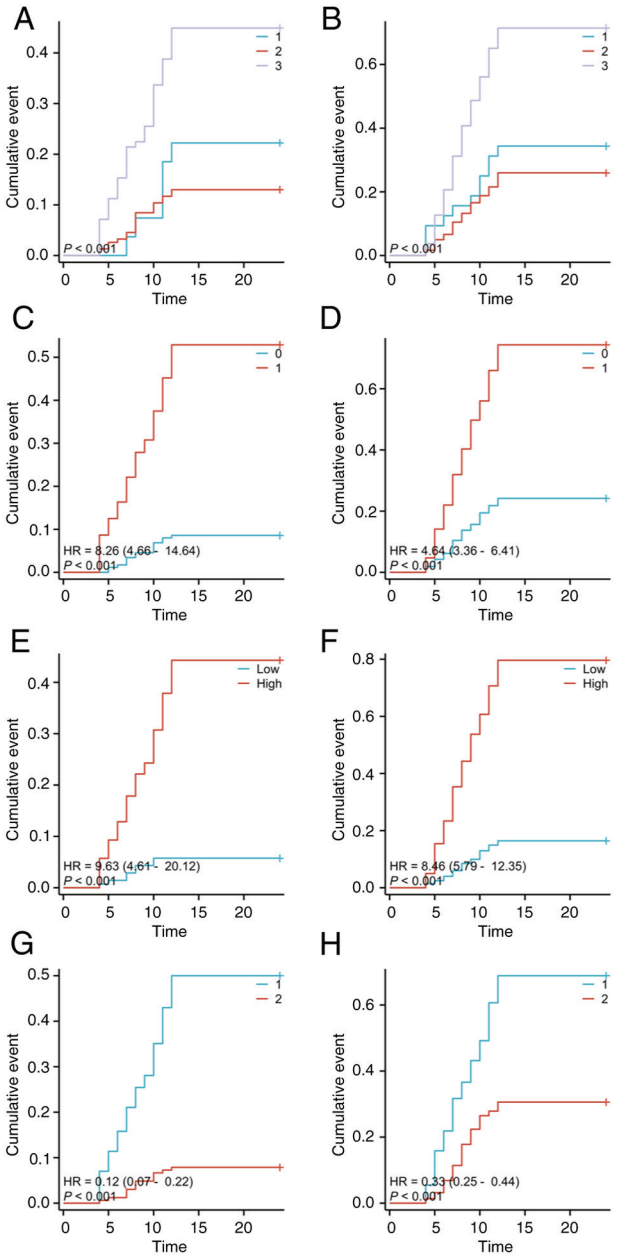

Figure 7. Kaplan-Meier curves of patients staged preoperatively as T_1, T_2 and T_3: (A) for grade 3+ pneumonia, (B) for grade 2-pneumonia. Preoperative staging as M_0, M_1: (C) for grade 3+ pneumonia, (D) for grade 2-pneumonia. Patients divided into high and low groups based on maximum dose >139,187.27 mCi, <139,187.27 mCi: (E) for grade 3+ pneumonia. Patients divided into high and low groups based on maximum dose >129,864.09 mCi, <129,864.09 mCi: (F) for grade 2-pneumonia. Grouping based on whether preoperative chemotherapy was administered (1 for yes, 2 for no): (G) for grade 3+ pneumonia, (H) for grade 2-pneumonia.

two, it was found that while the factors recognized in the present study's model focus more on the patient's individual biological characteristics, integrating these factors with the dosage and technical factors of EBRT could provide clinicians with a more comprehensive risk assessment tool. This multidimensional analysis can improve support of clinical decision-making and assist physicians in developing more personalized radiation therapy plans, thereby reducing the incidence of RP. Therefore, further exploring the relationships among these predictive factors will help expand the understanding of the mechanisms underlying RP and guide future research directions.

In conclusion, the findings of the present study contribute to the ongoing efforts to improve the prediction and management of radiation pneumonitis in patients undergoing brachytherapy with radioactive ^{125}I particles. Compared with existing models or guidelines, the present study's approach emphasizes multivariable analysis, which can consider the subtle differences in patients' individual characteristics and treatment plans. This personalized risk assessment method can assist clinicians in making more precise decisions when formulating treatment plans. In comparing with existing models, it was also noted that some commonly used risk assessment tools may be based solely on a single or few clinical characteristics, lacking a comprehensive consideration of multiple factors. The present study aimed to address this limitation by introducing more variables, thereby enhancing the predictive capability for the occurrence of RP. Through these comparisons, it was aimed to be demonstrated that the nomogram of the present study did not only improve accuracy but also assisted physicians in improving identification of high-risk patients in clinical applications, allowing for the formulation of more rational treatment plans.

The limitations of the present study include: i) Data completeness and accuracy: Retrospective studies rely on existing medical records and databases, the accuracy and completeness of which can be affected by various factors, such as data entry errors, missing information, or inconsistencies in recording treatment protocols. This may lead to some key variables being excluded from the analysis, potentially impacting the accuracy of the present study's predictive model. ii) Time effects: With advances in medical technology, the methods and standards of radiation therapy have evolved. In light of new treatment strategies and techniques, the data from retrospective studies may not reflect the true impact of radiation pneumonia risk in current clinical practice. This needs to be considered when applying the present study's findings to avoid generalizing outdated standards and results to modern treatments. iii) Limitations in inferring causality: Retrospective studies typically struggle to establish clear causal relationships. In the present study research, although several risk factors were identified to be associated with radiation pneumonia, this did not imply that these factors necessarily cause the occurrence of RP. The present study's findings need to be cautiously interpreted and the predictive nature of this mod emphasized rather than making causal judgments. iv) Inherent limitations of retrospective studies: The present study was a retrospective analysis and there may be biases in patient selection criteria and data collection. For instance, the selected patients may significantly differ from the general population (for example, age and tumor staging), which can affect the model's applicability. v) Limitations in variable selection: Even when using advanced methods such as LASSO for variable selection, important influencing factors may still be omitted, or unrelated variables may be included, thereby affecting the model's accuracy. vi) Lack of external validation: Ideally, validation should be conducted on external datasets to ensure the model's generalizability. However, the present study may lack sufficient external validation data.

Future research should continue to explore the interaction of various risk factors and dosimetric parameters to develop more effective strategies for preventing and treating this potentially debilitating complication of radiotherapy. In the present study, it was demonstrated that four independent risk factors (preoperative N and M staging, maximum dose and receipt of chemotherapy) can predict the occurrence of postoperative radiation pneumonitis in patients undergoing ^{125}I brachytherapy for cancer. The training cohort's area under the ROC curve for the nomogram construction was 0.878 (95% CI, 0.814-0.942), while the validation cohort's area under the ROC curve was 0.828 (95% CI, 0.787-0.870). The calibration curve indicates that the model can perfectly predict actual events. The DCA suggests that clinical decisions based on the predictive model are beneficial, implying practical clinical applicability and operability of the model. The maximum dose in both the training and validation cohorts revealed the most ideal clinical benefits in clinical practice, indicating promising clinical utility.

Integrating the nomogram into the existing clinical workflow can provide clinicians with a practical tool to aid in making more accurate patient care and treatment adjustment decisions. By showcasing real case studies that demonstrate the application of the nomogram in patient management, its value and effectiveness can be highlighted in clinical decision-making, helping physicians understand its importance. Effectively incorporating the nomogram into the existing clinical workflow will enhance clinicians' decision-making capabilities, offering patients more precise and personalized care and treatment adjustments. Combining educational training, system integration, standardized processes and multidisciplinary collaboration will be beneficial in achieving this goal, ultimately improving patient health outcomes. The feasible initiatives mainly include integrating it with Electronic Health Records for direct data access, developing a user-friendly interface for easy data entry, providing training for clinicians, embedding it into Clinical Decision Support Systems for risk-based recommendations, establishing feedback channels for continuous improvement, standardizing risk communication through clinical documentation, promoting collaboration among healthcare professionals, and regularly updating the nomogram based on new research. These efforts will ultimately enhance the effectiveness and application of the nomogram in clinical practice, leading to improved patient care outcomes.

Acknowledgements

Not applicable.

Funding

The present study was supported by Joint Plan of Liaoning Provincial People's Livelihood Science and Technology (grant no. 2022JH2/101500021).

Availability of data and materials

The data generated in the present study may be requested from the corresponding author.

Authors' contributions

GZ, SH and ZW contributed to the study conception and design. Material preparation, data collection and analysis were performed by TD and WZ. The first draft of the manuscript was written by TD. All authors read and approved the final version of the manuscript. TD and WZ confirm the authenticity of all the raw data.

Ethics approval and consent to participate

The study was reviewed and approved [approval no. YLS No. (2019) 69] by the Medical Ethics Committee of the General Hospital of Northern Theater Command in China (Shenyang, China). All patients provided signed informed consent.

Patient consent for publication

Not applicable.

Competing interests

The authors declare that they have no competing interests.

References

1. Huang M, Lin Q, Wang H, Chen J, Bai M, Wang L, Zhu K, Jiang Z, Guan S, Li Z, *et al*: Survival benefit of chemoembolization plus Iodine125 seed implantation in unresectable hepatitis B-related hepatocellular carcinoma with PVTT: A retrospective matched cohort study. Eur Radiol 26: 3428-3436, 2016.
2. Song J, Fan X, Zhao Z, Chen M, Chen W, Wu F, Zhang D, Chen L, Tu J and Ji J: ^{125}I brachytherapy of locally advanced non-small-cell lung cancer after one cycle of first-line chemotherapy: A comparison with best supportive care. Onco Targets Ther 10: 1345-1352, 2017.
3. Yang DY, Lin YP, Xue C, Fan JM, Wang Y, Cai C, Song DH and Zeng YM: CT-guided percutaneous implantation of ^{125}I particles in treatment of early lung cancer. J Thorac Dis 12: 5996-6009, 2020.
4. Wang H, Lu J, Zheng XT, Zha JH, Jing WD, Wang Y, Zhu GY, Zeng CH, Chen L and Guo JH: Oligorecurrence non-small cell lung cancer after failure of first-line chemotherapy: Computed tomography-guided ^{125}I seed implantation vs second-line chemotherapy. Front Oncol 10, 470, 2020.
5. Ji Z, Jiang Y, Guo F, Peng R, Sun H, Wang P, Fan J and Wang J: Radiation-related adverse effects of CT-guided implantation of ^{125}I seeds for thoracic recurrent and/or metastatic malignancy. Sci Rep 9: 14803, 2019.
6. Wang G, Zhang F, Yang B, Xue J, Peng S, Zhong Z, Zhang T, Lu M and Gao F: Feasibility and clinical value of CT-guided (125) I brachytherapy for bilateral lung recurrences from colorectal carcinoma. Radiology 278: 897-905, 2016.
7. Su L, Dong Y, Wang Y, Wang Y, Guan B, Lu Y, Wu J, Wang X, Li D, Meng A and Fan F: Potential role of senescent macrophages in radiation-induced pulmonary fibrosis. Cell Death Dis 12: 527, 2021.
8. Cai G, Liang S, Li C, Meng X and Yu J: Left ventricular systolic dysfunction is a possible independent risk factor of radiation pneumonitis in locally advanced lung cancer patients. Front Oncol 9: 1511, 2020.
9. Simeonova AO, Fleckenstein K, Wertz H, Frauenfeld A, Boda-Heggemann J, Lohr F and Wenz F: Are three doses of stereotactic ablative radiotherapy (SABR) more effective than 30 doses of conventional radiotherapy? Transl Lung Cancer Res 1: 45-53, 2012.
10. Zheng RS, Chen R, Han BF, Wang SM, Li L, Sun KX, Zeng HM, Wei WW and He J: Cancer incidence and mortality in China, 2022. Zhonghua Zhong Liu Za Zhi 46: 221-231, 2024 (In Chinese).

11. Münsterberg J, Loreth D, Brylka L, Werner S, Karbanova J, Gandrass M, Schneegans S, Besler K, Hamester F, Robador JR, *et al*: ALCAM contributes to brain metastasis formation in non-small-cell lung cancer through interaction with the vascular endothelium. Neuro Oncol 22: 955-966, 2020.
12. Wang Y, Zhu L, Lin X, He C, An Z, Tang J, Lv W and Hu J: Therapeutic effect of CT-guided ^{125}I seed implantation on advanced lung cancer and pulmonary metastatic carcinoma. Zhongguo Fei Ai Za Zhi 23: 424-428, 2020 (In Chinese).
13. Wang X and Wang D: Clinical analysis of 125I seed implantation combined with epidermal growth factor receptor-tyrosine kinase inhibitors in advanced non-small cell lung cancer. J BUON 26: 1879-1886, 2021.
14. Zhang T, Lu M, Peng S, Zhang W, Yang G, Liu Z, Singh S, Yang Y, Zhang F and Gao F: CT-guided implantation of radioactive 125I seed in advanced non-small-cell lung cancer after failure of first-line chemotherapy. J Cancer Res Clin Oncol 140: 1383-1390, 2014.
15. Cao X, Fang L, Cui CY, Gao S and Wang TW: DTI and pathological changes in a rabbit model of radiation injury to the spinal cord after ^{125}I radioactive seed implantation. Neural Regen Res 13: 528-535, 2018.
16. Zha Y, Zhang J, Yan X, Yang C, Wen L and Li M: A dynamic nomogram predicting symptomatic pneumonia in patients with lung cancer receiving thoracic radiation. BMC Pulm Med 24: 99, 2024.
17. De Petris L, Lax I, Sirzén F and Friesland S: Role of gross tumor volume on outcome and of dose parameters on toxicity of patients undergoing chemoradiotherapy for locally advanced non-small cell lung cancer. Med Oncol 22: 375-381, 2005.
18. Yu X, Li J, Zhong X and He J: Combination of Iodine-125 brachytherapy and chemotherapy for locally recurrent stage III non-small cell lung cancer after concurrent chemoradiotherapy. BMC Cancer 15: 656, 2015.
19. Takeda A, Tsurugai Y, Sanuki N, Enomoto T, Shinkai M, Mizuno T, Aoki Y, Oku Y, Akiba T, Hara Y and Kunieda E: Clarithromycin mitigates radiation pneumonitis in patients with lung cancer treated with stereotactic body radiotherapy. J Thorac Dis 10: 247-261, 2018.
20. Bi J, Meng R, Yang D, Li Y, Cai J, Zhang L, Qian J, Xue X, Hu S, Yuan Z, *et al*: Dosimetric predictors of radiation pneumonitis in patients with prior immunotherapy exposure: A multi-institutional analysis. Radiother Oncol 190: 110040, 2024.
21. Ji Z, Ni Y, He C, Huo B, Liu S, Ma Y, Song Y, Hu M, Zhang K, Wang Z, *et al*: Clinical outcomes of radioactive seed brachytherapy and microwave ablation in inoperable stage I non-small cell lung cancer. Am J Cancer Res 13: 3753-3762, 2023.
22. Flakus MJ, Kent SP, Wallat EM, Wuschner AE, Tennant E, Yadav P, Burr A, Yu M, Christensen GE, Reinhardt JM, *et al*: Metrics of dose to highly ventilated lung are predictive of radiation-induced pneumonitis in lung cancer patients. Radiother Oncol 182: 109553, 2023.
23. Huang P and Yi X: Risk factors and a model for prognosis prediction after intravenous thrombolysis with alteplase in acute ischemic stroke based on propensity score matching. Int J Immunopathol Pharmacol 38: 3946320241274231, 2024.